



Published in final edited form as:

Circ Genom Precis Med. 2022 October ; 15(5): e003238. doi:10.1161/CIRCGEN.120.003238.

Acacetin, a Potent Transient Outward Current Blocker, May Be a Novel Therapeutic for *KCND3*-Encoded Kv4.3 Gain-of-Function-Associated J-Wave Syndromes

Dan Ye, MD^{1,*}, Wei Zhou, MD^{1,*}, Samantha K. Hamrick, BS¹, David J Tester, BS¹, CS John Kim, PhD¹, Hector Barajas-Martinez, PhD², Dan Hu, MD, PhD³, John R. Giudicessi, MD, PhD¹, Charles Antzelevitch, PhD², Michael J. Ackerman, MD, PhD¹

¹Department of Molecular Pharmacology & Experimental Therapeutics (Windland Smith Rice Sudden Death Genomics Laboratory); Department of Cardiovascular Medicine/Division of Heart Rhythm Services (Windland Smith Rice Genetic Heart Rhythm Clinic); Department of Pediatric and Adolescent Medicine/Division of Pediatric Cardiology, Mayo Clinic, Rochester, MN;

²Lankenau Institute for Medical Research, Wynnewood, PA;

³Department of Cardiology and Cardiovascular Research Institute, Renmin Hospital of Wuhan University, Wuhan, China

Abstract

Background: The transient outward current (I_{to}) that mediates early (phase 1) repolarization is conducted by the *KCND3*-encoded Kv4.3 pore-forming α -subunit. *KCND3* gain-of-function mutations have been reported previously as a pathogenic substrate for J wave syndromes (JWS), including the Brugada syndrome (BrS) and Early Repolarization syndrome (ERS), as well as autopsy-negative sudden unexplained death (SUD). Acacetin, a natural flavone, is a potent I_{to} current blocker. Acacetin may be a novel therapeutic for *KCND3*-mediated JWS.

Methods: *KCND3*-V392I was identified in an 18-year-old male with JWS/ERS, and a history of cardiac arrest including ventricular tachycardia/ventricular fibrillation and atrial fibrillation/atrial flutter. Pathogenic *KCND3* mutation was engineered by site directed mutagenesis and co-expressed with wild type KChIP2 in TSA201 cells. Gene-edited/variant-corrected isogenic control and patient-specific pluripotent stem cell-derived cardiomyocytes (iPSC-CMs) from the p. Val392Ile-*KCND3*-positive patient were generated. I_{to} currents and action potentials (APs) were recorded before and after treatment with Acacetin using the whole cell patch-clamp and multielectrode array (MEA) technique. Western blot and immunocytochemistry were performed to investigate *KCND3* expression.

Correspondence: Michael J. Ackerman, MD, PhD, Mayo Clinic Windland Smith Rice Sudden Death Genomics Laboratory, Guggenheim 501, Mayo Clinic, 200 First Street SW, Rochester, MN 55905, Tel: 507-284-0101, Fax: 507-284-3757, mackerman.michael@mayo.edu.

*co-equal first authors

Supplemental Materials:
Supplemental Methods
Supplemental Tables I–IV
Supplemental Figure I

Results: KCND3-V392I demonstrated a marked gain-of-function phenotype, increasing peak I_{to} current density by 92.2% ($p < 0.05$ vs. KCND3-WT). KCND3 expression was significantly increased in KCND3-V392I-derived iPSC-CMs ($p < 0.05$ vs. isogenic control). While KCND3-WT revealed an IC_{50} of $7.2 \pm 1.0 \mu M$ for Acacetin effect, $30 \mu M$ Acacetin dramatically inhibited KCND3-V392I peak I_{to} current density by 96.2% ($p < 0.05$ vs. before Acacetin). I_{to} was also increased by 60.9% in Kv4.3-V392I iPSC-CM ($p < 0.05$ vs. isogenic control iPSC-CM). $10 \mu M$ Acacetin, a concentration approaching its IC_{50} value, inhibited I_{to} by approximately 50% in patient-derived iPSC-CMs and reduced the accentuated AP notch displayed in KCND3-V392I-derived iPSC-CMs.

Conclusions: This pre-clinical study provides pharmacological and functional evidence to suggest that Acacetin may be a novel therapeutic for patients with KCND3 gain-of-function-associated JWS by inhibiting I_{to} and abolishing the accentuated AP notch in patient-derived iPSC-CMs.

Keywords

Acacetin; Arrhythmia; J Wave Syndrome/ Early Repolarization Syndrome; Gene mutation; Ion channel

Introduction

The transient outward current (I_{to}) is a rapidly activating potassium channel current that is responsible for phase 1 of the cardiac action potential. I_{to} is produced by *KCND3*-encoded Kv4.3 channels. *KCND3* gain-of-function mutations generate a pathogenic substrate responsible for the J wave syndromes (JWS), including the Brugada syndrome (BrS)¹ and Early Repolarization syndrome (ERS)², as well as autopsy-negative sudden unexplained death (SUD)³.

The J point denotes the junction of the QRS complex and the ST segment on the ECG, marking the end of depolarization and the beginning of repolarization. The term J wave or Osborn wave denotes an elevated J-point or ST-segment elevation immediately following the QRS complex of the surface ECG^{4, 5}. A prominent I_{to} -mediated action potential notch in ventricular epicardium but not endocardium produces a transmural voltage gradient during early ventricular repolarization that registers as a J wave or J-point elevation on the ECG⁴. We refer to the “syndrome” when a J wave pattern in the ECG is accompanied by clinical symptoms including arrhythmic manifestations and sudden cardiac death⁶. JWS were proposed as a unifying definition for 2 clinical entities, namely BrS and ERS^{5, 6}. BrS and ERS have similar cellular and genetic pathophysiology underlying the genesis of arrhythmias secondary to and outward shift in the balance of current in the early phases of the ventricular action potential. The resulting defects give rise to closely coupled extrasystoles via a “phase 2 reentry” mechanism, which in turn precipitates polymorphic ventricular tachycardia and/or fibrillation (VT/VF). The outward shift in the balance of current can be due to reduced inward currents, such as sodium or calcium currents or to increased I_{to} or ATP-dependent potassium current (K_{ATP})^{5, 6}. The imbalance between depolarizing and repolarizing forces in the early phase of cardiac action potential (AP) is the

current hypothesis for the generation of a pathologic J wave in the right ventricular outflow tract (RVOT) in the case of BrS or in the inferior/lateral wall in the case of ERS^{5 6}.

Implantation of a cardioverter-defibrillator (ICD) is an effective therapeutic strategy for those JWS patients with either resuscitated sudden cardiac arrest (SCA) or arrhythmic syncope⁵. However, an ICD may be problematic in infants or young children because of the high complication rate⁵. Quinidine by virtue of its effect to inhibit I_{to} effectively prevents/reduces ventricular fibrillation (VF) in patients with BrS as well as ERS and has proven to be an alternative to ICD therapy^{7, 8}. Owing to its action to inhibit I_{Kr} , quinidine predisposes to the development of QT interval prolongation and the development of life-threatening Torsade de Pointes arrhythmias⁹. These actions of quinidine have prompted the search for other pharmacologic approaches to the treatment of JWS.

Acacetin, a natural flavone effectively blocks human atrial ultra-rapidly delayed rectifier potassium (I_{Kur}), acetylcholine-activated potassium (I_{K-ACh}), and I_{to} currents and therefore has been viewed as a promising agent for the treatment of atrial fibrillation (AF)¹⁰. Since I_{Kur} and I_{K-ACh} are expressed at negligible levels in ventricular myocardium, we hypothesize that acacetin, may function as an I_{to} specific channel blocker in the ventricles and serve as a novel therapeutic for JWS caused by an increased, unopposed Ito current in the ventricular epicardium.

As such, in the present study, we investigated the potential Ito-blocking effects of Acacetin in TSA201 cells heterologously expressing a *KCND3* gain-of-function variant (p. Val392Ile-KCND3) as well as patient-specific pluripotent stem cell-derived cardiomyocytes (iPSC-CMs) from a p. Val392Ile-KCND3-positive patient with recurrent ventricular arrhythmias and a clinical diagnosis of JWS-ERS subtype.

Methods

Written informed consent was obtained for this Mayo Clinic Institutional Review Board approved study (09–006465). The data that support the findings of this study are available from the corresponding author upon reasonable request. A full description of methods, including drug and statistical analysis are available in supplemental material.

Case Report

An 18-year-old adopted male of Asian descent with an unremarkable medical history aside from three “febrile seizures” during early childhood presented to a local emergency department after suffering a witness collapsed with seizure-like activity while camping outdoors with his family. Preceding his collapse, the patient awoke from sleep with extreme dizziness, diaphoresis, and nausea and vomiting and alerted his mother. In the local emergency department, the patient once again lost consciousness and seizure-like activity was noted. On telemetry, polymorphic ventricular tachycardia/ventricular fibrillation (VF) was noted (Figure 1A). After a pulse was subsequently lost, cardiopulmonary resuscitation (CPR) was initiated promptly and spontaneous return of circulation achieved following several rounds of CPR and six external defibrillator shocks.

Following his in-hospital cardiac arrest, the patient was admitted and immediate post-SCA work-up was remarkable for serial 12-lead ECGs displaying global and inferolateral global J point elevation and paroxysmal atrial flutter (Figure 1B and 1C). Prior to discharge, the patient received a dual-chamber ICD for secondary prevention.

Due to concerns for possible BrS, the patient was referred to the Mayo Clinic Windland Smith Rice Genetic Heart Rhythm Clinic and subsequently underwent commercial BrS/ERS genetic testing which identified a likely pathogenic variant (p. Val392Ile-KCND3) that localizes to the transmembrane domain of the Kv4.3 voltage-gate potassium channel (Figure 1D). Importantly, p. Val392Ile-KCND3 was identified previously in a young SUD victim, found to confer an *in vitro* gain-of-function electrophysiological phenotype, and is the only putative BrS/SUD-associated *KCND3* genetic variant absent in the Genome Aggregation Database (gnomAD) of public exomes/genomes³.

Of note, the patient's first post-discharge device interrogation revealed two episodes of atrial fibrillation/atrial flutter shortly after discharge. Over the next three years, there were several episodes of symptomatic atrial flutter with rapid ventricular response and one inappropriate ICD shock due to T-wave over sensing.

Unfortunately, roughly four years after his sentinel in-hospital cardiac arrest, the patient received an appropriate VF-terminating ICD shock while sleeping (Figure 1E). Given concern for p. Val392Ile-KCND3-mediated ERS (i.e., Ito gain-of-function), the patient was admitted and loaded with quinidine. However, approximately one week after quinidine was initiated, the patient developed nausea and diffuse muscle aches. Work-up at this time revealed elevated liver enzymes and due to concern for quinidine-induced lupus, quinidine was held with subsequent resolution of both symptoms and transaminitis. In this setting, the patient experienced a second appropriate ventricular fibrillation-terminating ICD shock while sleeping (Figure 1F). He was again admitted and continued to have episodes of short-coupled torsades de pointes/premature ventricular contraction (PVC)-triggered VF.

With limited viable pharmacologic options, the patient ultimately underwent a PVC-targeted ablation as the inciting PVC was felt to be originating from the left posterior fascicle and was discharged subsequently on mexiletine. However, he experienced two additional appropriate VF-terminating ICD shocks over a 48-hour period and was once again admitted. After considerable discussion, the decision was ultimately made to trial flecainide for PVC suppression. In the event that flecainide was unsuccessful or exacerbated the patient's underlying genetic substrate, patient-specific iPSC-CMs were generated to produce a "disease in the dish" model for which experimental agents such as Acacetin could be tested for therapeutic efficacy *in vitro* before consideration of compassionate use in the patient should the need arise.

Results

KCND3-V392I was reported previously as a gain-of-function variant in a sudden death patient³. Acacetin is a potent I_{to} channel blocker¹¹. In order to examine the optimal concentration for acacetin, we performed a dose-response assessment of the effect of

Acacetin to block I_{to} in HEK293 cells transfected with WT or mutant KCND3 together with KChIP2-WT. Figure 2A shows representative I_{to} traces recorded before and after exposure to 7.5 μM Acacetin. Acacetin blocked I_{to} in a concentration –dependent manner with an IC_{50} of $7.2 \pm 1.0 \mu\text{M}$ ($n=3-5$) (Figure 2B). Previous studies revealed that 30 μM Acacetin potently blocked Kv4.3-WT and variants in segment 6, V392A, I395A and V399A¹¹. Here, we tested whether 30 μM Acacetin has similar effects on I_{to} in Kv4.3-WT as well as channels expressing the gain-of-function variant, V392I in TSA201 cells.

Consistent with our previous report³, Kv4.3-V392I plus KChIP2 increased I_{to} current, whereas perfusion of 30 μM Acacetin dramatically blocked Kv4.3-WT and V392I I_{to} channels (Figure 2C). Analysis of the current-voltage relationship indicated that Kv4.3-V392I plus KChIP2-WT significantly increased I_{to} density from –10 mV to +40 mV ($n=10$, $p<0.05$) compared with Kv4.3-WT plus KChIP2-WT ($n=8$, Figure 2D). At +40 mV, I_{to} density was increased significantly by 92.2% from $530.8 \pm 132.2 \text{ pA/pF}$ (WT, $n=8$) to $1020.3 \pm 143.4 \text{ pA/pF}$ (V392I, $n=10$, $p=0.026$) (Figure 2E). 30 μM Acacetin almost completely blocked Kv4.3-WT and V392I current from –30 mV to +40 mV ($p<0.05$ vs. before Acacetin) reaching a level of $42.8 \pm 7.9 \text{ pA/pF}$ (WT at +40 mV, $n=8$, $p=0.0079$ vs. before Acacetin) and $39.1 \pm 7.1 \text{ pA/pF}$ (V392I at +40 mV, $n=10$, $p<0.0001$ vs. before Acacetin) respectively (Figure 2D, 2E).

In order to examine whether an I_{to} gain-of-function is observed in Kv4.3-V392I iPSC-CMs and the effect of Acacetin, we recorded I_{to} in iPSC-CMs derived from the Kv4.3-V392I patient and gene-edited/variant-corrected isogenic control cell lines. Similar to the findings in TSA201 cells, I_{to} was greater in Kv4.3-V392I iPSC-CM compared to the isogenic control (Figure 3). At +40 mV, I_{to} density was 60.9% greater in iPSC-CMs from $20.2 \pm 2.6 \text{ pA/pF}$ (isogenic control, $n=10$) to $32.5 \pm 4.6 \text{ pA/pF}$ (V392I, $n=11$, $p=0.034$ vs. isogenic control) (Figure 3C). 10 μM Acacetin, a concentration approaching its IC_{50} value, significantly inhibited I_{to} by 53.8% ($n=11$, $p=0.0028$ vs. before Acacetin) and 39.1% ($n=10$, $p=0.0004$ vs. before Acacetin) in case- and isogenic control-derived iPSC-CMs respectively.

To investigate whether KCND3 expression level is altered in KCND3-V392I-derived iPSC-CMs and where KCND3 is located, we carried out western blot and immunofluorescence study on iPSC-CMs. Our data showed KCND3 expression relative to vinculin was significantly increased in KCND3-V392I iPSC-CMs (2.1 ± 0.18 , $n=6$) compared with that in control (1 ± 0.20 , $n=6$, $p=0.0087$) (Figure 4A, 4B). KCND3 was located in nucleus, plasma membrane (images on the left panel, Figure 4C), endoplasmic reticulum (images on the right panel, Figure 4C), and KCND3 fluorescent intensity was significantly increased in KCND3-V392I-derived iPSC-CMs ($44.4 \pm 2.1 \text{ A.U.}$, $n=201$) compared with the control cells ($27.4 \pm 1.1 \text{ A.U.}$, $p<0.0001$) (Figure 4D).

Next, we tested whether I_{to} gain-of-function caused by Kv4.3-V392I could demonstrate pro-arrhythmic activities in patient cells using patch clamp current configuration. Action potential (AP) measurements were performed in both isogenic control and Kv4.3-V392I-derived iPSC-CMs. Interestingly, Kv4.3-V392I-iPSC-CMs (not isogenic control-derived iPSC-CMs) revealed an accentuated AP notch. Not surprisingly, 10 μM Acacetin reduced the AP notch, restored AP dome in Kv4.3-V392I-derived iPSC-CMs indicating its potential

anti-arrhythmic effect (Figure 5A). However, action potential duration (APD50 and APD90) remained unchanged between isogenic control and Kv4.3-V392I-derived iPSC-CMs before the treatment of Acacetin. 10 μ M Acacetin did not affect APD50 and APD90 in both isogenic control and Kv4.3-V392I-derived iPSC-CMs (Figure 5B, 5C) (Supplemental Table III in Supplemental material).

Since I_{to} current and AP phase 1 notch were not displayed in every iPSC-CM, it is hard to obtain enough pro-arrhythmic activities using patch clamp assay for statistical analysis. To confirm whether KCND3-V392I could induce increased phase I notch, and whether Acacetin could abolish this increased phase I notch, we used a high-throughput assay, the LEAP technology, to quantify action potential phase I notch. Our data showed that there were 16.7% of phase I notch-like traces in KCND3-V392I iPSC-CMs compared with 3.3% in isogenic control cells (56 out of 335 vs. 14 out of 422 respectively, $p=0.00001$). After treatment of KCND3-V392I iPSC-CMs with 10 μ M of Acacetin for 30 min, phase I notch-like traces were reduced to 11.0% (58 out of 528, $p=0.016$ vs. before Acacetin) (Figure 6A, 6B). Consistent with patch clamp AP measurements, Acacetin didn't affect APD30, APD50 and APD90 when using MEA assay (Figure 6A, 6C) (Supplemental Table IV in Supplemental material).

Discussion

The JWSs, consisting of BrS and ERS, have captured the interest of the cardiology community over the past 2 decades and are associated with vulnerability to development of polymorphic VT and VF leading to SCD⁵. BrS can be diagnosed in the presence of a “type 1 Brugada ECG,” consisting of a J-point elevation ≥ 2 mm with descending ST segment and negative T wave in the right precordial leads V1 and V2. ERS is generally diagnosed in patients who display ER in the inferior and/or lateral leads presenting with aborted cardiac arrest, documented VF, or polymorphic VT with ER defined as the presence of (1) an end-QRS notch or slur on the downslope of a prominent R wave. The notch/slur should be entirely above the baseline. (2) A peak of the J wave (notched or slurred) ≥ 0.1 mV in 2 or more contiguous leads of the 12-lead ECG, excluding leads V1 to V3^{5,6}.

Kv4.3-V392I was first reported in a 20-year-old male autopsy-negative sudden death victim without any premortem ECGs and a negative family history of sudden death or arrhythmia-related cardiac events³. Here, we reported Kv4.3-V392I mutation in an adopted 18-year-old patient diagnosed clinically as ERS with the J-point elevation in serial 12-lead ECGs displaying global and inferolateral global J point elevation and polymorphic VT, VF, atrial fibrillation and atrial flutter. Our patch clamp studies revealed increased levels of I_{to} in both TSA201 cells transfected with KCND3-V392I and iPSC-CMs derived from the patient with the KCND3-V392I variant, which is consistent with our previous findings. Further, our western blot study revealed that KCND3 expression was increased in KCND3-V392I-derived iPSC-CMs compared with control iPSC-CMs. Immunofluorescence study exhibited that KCND3 was localized in nucleus, cytosol, endoplasmic reticulum and plasma membrane. KCND3 fluorescent intensity was also increased in KCND3-V392I iPSC-CMs indicating KCND3 expression was accentuated in patient cells. These two findings supported that our I_{to} gain-of-function observed in patch clamp study was mainly

due to a biogenic increase in *KCND3* expression, rather than a biophysical gain-of-function in the *KCND3*-encoded Kv4.3 channels from the patient with the *KCND3*-V392I variant.

Our group previously reported that gain-of-function pathogenic variants in *KCND3* can serve as a pathogenic substrate for BrS¹. Since BrS and ERS have similar cellular and genetic pathophysiology for the genesis of arrhythmias⁵, our findings point to the gain of function of I_{to} caused by the *KCND3*-V392I mutation as providing the pathogenic substrate in this patient diagnosed with JWS/ERS.

Acacetin is a flavone compound (5, 7-dihydroxy-4-methoxyflavone) that is broadly distributed in plant pigments and responsible for many of the colors in nature¹⁰. Acacetin blocks the Kv1.3 channel, inhibits human T cell activation, and serves as an attractive therapeutic target to treat inflammatory and immunological disorders¹². Acacetin suppresses I_{Kur} , I_{ACh} and I_{to} thereby prolonging the action potential duration in human atrial myocytes without affecting sodium, L-type calcium, or inward-rectifier potassium currents in guinea pig cardiac myocytes. Although Acacetin causes a weak reduction in hERG and hKCNQ1/hKCNE1 channels stably expressed in HEK 293 cells, it did not prolong the corrected QT interval in rabbit hearts. In anesthetized dogs, Acacetin is reported to prolong the atrial effective refractory period without prolonging the corrected QT interval and to effectively prevent atrial fibrillation (AF)¹⁰.

Acacetin inhibits hKv4.3 channels by binding to their P-loop filter helix and S6 domain at both the closed and open state of the channels and decreases the recovery from inactivation¹¹. Blockade of hKv4.3 wild type channel by Acacetin is use- and frequency-dependent with IC_{50} of 7.9 μ M. hKv4.3 mutants T366A and T367A affecting the P-loop helix, and V392A, I395A and V399A affecting the S6-segment have been shown to reduce channel blocking efficacy of Acacetin (IC_{50} , 44.5 μ M for T366A, 25.8 μ M for T367A, 17.6 μ M for V392A, 16.2 μ M for I395A, and 19.1 μ M for V399A)¹¹.

Here, we report blockade of Kv4.3-WT I_{to} by Acacetin with IC_{50} of 7.2 μ M in HEK293 cells. In order to examine whether *KCND3*-V392I causes reduced efficacy of I_{to} block effect by Acacetin, we utilized 30 μ M concentration which was close to the IC_{50} of Acacetin for previously reported *KCND3* variants located in S6-segment. Surprisingly, 30 μ M Acacetin almost completely inhibited I_{to} carried by WT Kv4.3 channels as well as mutant Kv4.3 channels (V392I - located in the S6-segment) in which the current exhibited a prominent gain of function. In order to test whether a 10 μ M IC_{50} concentration of Acacetin might be appropriate to treat this patient, we generated isogenic control iPSC-CMs and patient-derived iPSC-CMs harboring the *KCND3*-V392I pathogenic variant. We found that 10 μ M Acacetin inhibited I_{to} by approximately 50% in iPSC-CMs from the *KCND3*-V392I-positive patient and approximately 40% from isogenic control iPSC-CMs. In the patient-derived iPSC-CMs, Acacetin brought I_{to} back to normal levels, thus correcting the gain-of-function caused by the pathogenic variant.

Recently, Di Diego et al reported that Acacetin (5–10 μ M) reduced I_{to} density, AP notch and J wave area and totally suppressed the electrocardiographic and arrhythmic manifestation of both BrS and ERS. In wedge and whole-heart models of JWS, increasing I_{to} with

NS5806, decreasing I_{Na} or I_{Ca} (with ajmaline or verapamil) or hypothermia all resulted in accentuation of epicardial AP notch and ECG J waves, resulting in characteristic BrS and ERS phenotypes. All repolarization defects giving rise to VT/VF in the BrS and ERS models were reversed by acacetin, resulting in total suppression of VT/VF indicating Acacetin as a promising new pharmacologic treatment for JWS¹³. Here, we report that KCND3-V392I-derived iPSC-CMs demonstrated accentuated AP notch, whereas 10 μ M Acacetin corrected the increased AP notch and reduced the total number of AP notches observed in patient-derived iPSC-CMs harboring the KCND3-V392I pathogenic variant without affecting APD which was similar to the findings observed in the pharmacological mimic-JWS animal model¹³. These findings suggest that this action of Acacetin to reduce I_{to} may be of therapeutic benefit by producing an inward shift in the balance of current in the early phases of the epicardial action potential, thus reversing the substrate responsible for the development of prominent J waves that reflect the substrate for development of phase 2 reentry and VT/VF⁴. Acacetin may thus serve as a novel therapeutic for both BrS and ERS providing an alternative to quinidine for these sudden death syndromes and avoiding the development of QT interval prolongation and the development of life-threatening Torsade de Pointes arrhythmias induced by quinidine⁹. Besides VT/VF, this patient also presented atrial fibrillation and atrial flutter. Since Acacetin prolonged the atrial effective refractory period without prolonging the corrected QT interval which has been shown to effectively prevent atrial fibrillation¹⁰, this compound may benefit this patient with atrial arrhythmias treatment as well. However, because our patient has remained event free, we have not yet pursued compassionate use status of Acacetin.

Conclusions

This pre-clinical study provides pharmacological and functional evidence to suggest that Acacetin may be a novel therapeutic for patients with JWS particular those stemming from KCND3 gain of function by inhibiting I_{to} and abolishing the accentuated AP notch in patient-derived iPSC-CMs harboring KCND3 gain-of-function pathogenic variant.

Supplementary Material

Refer to Web version on PubMed Central for supplementary material.

Acknowledgments:

This work was supported by the Mayo Clinic Windland Smith Rice Comprehensive Sudden Cardiac Death Program.

Sources of Funding:

Supported by NIH grants HL47678, HL138103, HL152201 (CA), W.W. Smith Trust (CA) and the Wistar and Martha Morris Fund (CA).

Disclosures:

Dr. Ackerman is a consultant for Abbott, ARMGO Pharma, Boston Scientific, Daiichi Sankyo, Invitae, LQT Therapeutics, Medtronic, and UpToDate. Dr. Ackerman and Mayo Clinic are involved in an equity/royalty relationship with AliveCor, Anuman, and Pfizer. These relationships are all modest, and none of these entities have contributed to this study in any manner. Dr. Antzelevitch is a consultant to Trevena Pharmaceuticals,

Novartis Institutes for BioMedical Research and Praxis Pharmaceuticals and has received grant funds from Trevena Pharmaceuticals and Novartis Institutes for BioMedical Research. The other authors report no conflicts.

Nonstandard Abbreviations and Acronyms:

Ito	The transient outward current
JWS	J wave syndromes
BrS	Brugada syndrome
ERS	Early Repolarization syndrome
SUD	autopsy-negative sudden unexplained death
iPSC-CMs	pluripotent stem cell-derived cardiomyocytes
AP	action potential
VT/VF	ventricular tachycardia and/or fibrillation
K_{ATP}	ATP-dependent potassium current
RVOT	right ventricular outflow tract
ICD	implantation of a cardioverter-defibrillator
SCA	sudden cardiac arrest
I_{Kur}	ultra-rapidly-delayed rectifier potassium
I_{K-ACh}	acetylcholine-activated potassium
AF	atrial fibrillation
CPR	cardiopulmonary resuscitation
gnomAD	Genome Aggregation Database
PVC	premature ventricular contraction

References:

1. Giudicessi JR, Ye D, Tester DJ, Crotti L, Mugione A, Nesterenko VV, Albertson RM, Antzelevitch C, Schwartz PJ, and Ackerman MJ. Transient outward current (I_{to}) gain-of-function mutations in the KCND3-encoded Kv4.3 potassium channel and Brugada syndrome. *Heart Rhythm*. 2011; 8:1024–1032. [PubMed: 21349352]
2. Antzelevitch C. Genetic, molecular and cellular mechanisms underlying the J wave syndromes. *Circ J*. 2012; 76:1054–1065. [PubMed: 22498570]
3. Giudicessi JR, Ye D, Kritzberger CJ, Nesterenko VV, Tester DJ, Antzelevitch C, Ackerman MJ. Novel mutations in the KCND3-encoded Kv4.3 K⁺ channel associated with autopsy-negative sudden unexplained death. *Hum Mutat*. 2012; 33:989–997. [PubMed: 22457051]
4. Antzelevitch C and Yan GX. J wave syndromes. *Heart Rhythm*. 2010; 7:549–558. [PubMed: 20153265]

5. Antzelevitch C, Yan GX, Ackerman MJ, Borggrefe M, Corrado D, Guo J, Gussak I, Hasdemir C, Horie M, Huikuri H et al. J-Wave syndromes expert consensus conference report: Emerging concepts and gaps in knowledge. *Europace*. 2017; 19:665–694. [PubMed: 28431071]
6. Priori SG and Napolitano C. J-Wave Syndromes: Electrocardiographic and Clinical Aspects. *Card Electrophysiol Clin*. 2018; 10:355–369. [PubMed: 29784488]
7. Belhassen B, Glick A and Viskin S. Efficacy of quinidine in high-risk patients with Brugada syndrome. *Circulation*. 2004; 110:1731–1737. [PubMed: 15381640]
8. Yan GX and Antzelevitch C. Cellular basis for the Brugada syndrome and other mechanisms of arrhythmogenesis associated with ST-segment elevation. *Circulation*. 1999; 100:1660–1666. [PubMed: 10517739]
9. Barrows B, Cheung K, Bialobrzeski T, Foster J, Schulze J and Miller A. Extracellular potassium dependency of block of HERG by quinidine and cisapride is primarily determined by the permeant ion and not by inactivation. *Channels*. 2009; 3:4, 240–249.
10. Li GR, Wang HB, Qin GW, Jin MW, Tang Q, Sun HY, Du XL, Deng XL, Zhang XH, Chen JB et al. Acacetin, a natural flavone, selectively inhibits human atrial repolarization potassium currents and prevents atrial fibrillation in dogs. *Circulation*. 2008; 117:2449–2457. [PubMed: 18458165]
11. Wu HJ, Sun HY, Wu W, Zhang YH, Qin GW and Li GR. Properties and molecular determinants of the natural flavone acacetin for blocking hKv4.3 channels. *PLoS One*. 2013; 8: e57864. [PubMed: 23526953]
12. Zhao N, Dong Q, Fu XX, Du LL, Cheng X, Du YM, Liao YH. Acacetin blocks kv1.3 channels and inhibits human T cell activation. *Cell Physiol Biochem*. 2014; 34:1359–1372. [PubMed: 25301362]
13. Di Diego JM, Patocskaï B, Barajas-Martinez H, Borbáth V, Ackerman MJ, Burashnikov A, Clatot J, Li GR, Robinson VM, Hu D et al. *PLoS One*. 2020; Nov 24;15(11): e0242747. [PubMed: 33232375]

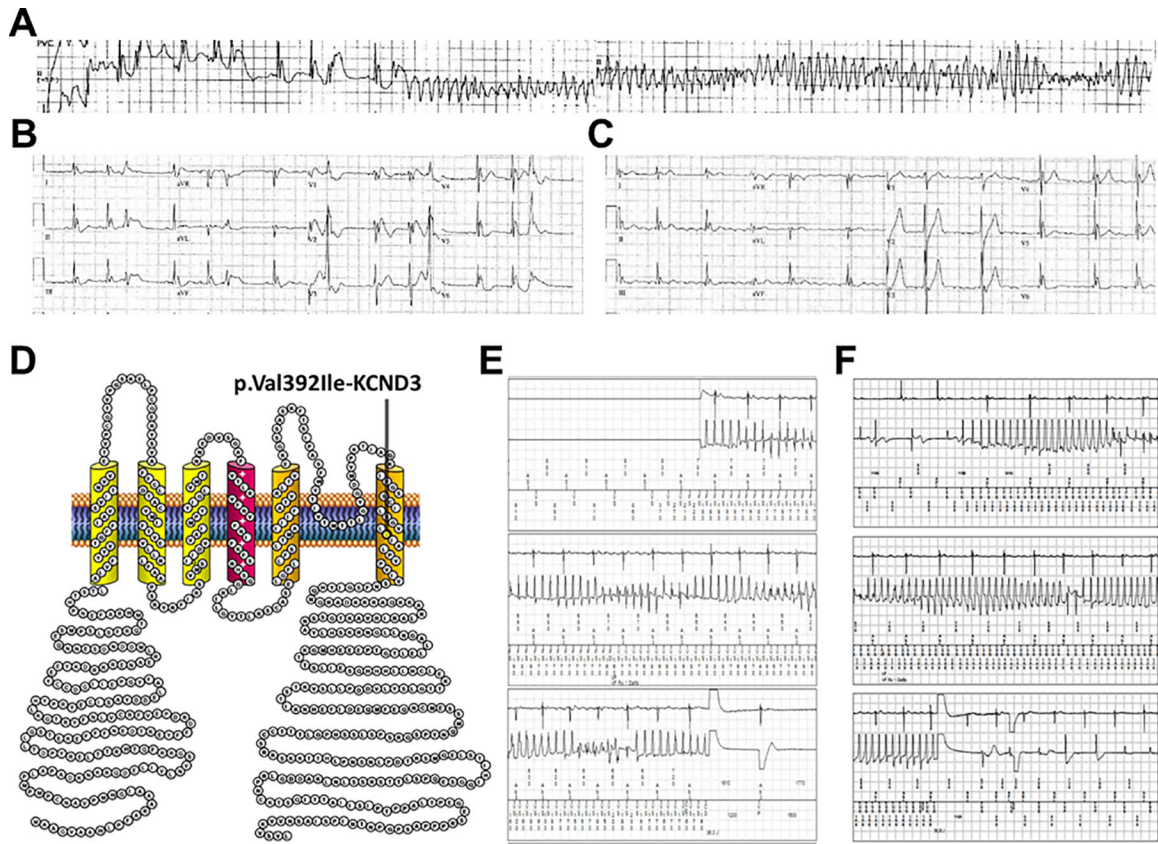


Figure 1.

Electrographic findings observed in a p. Val392Ile-KCND3-positive patient with a J-wave spectrum disorder. **A.** Telemetry rhythm strips obtained during resuscitation efforts after the p. Val392Ile-KCND3-positive patient experienced an in-hospital cardiac arrest. **B.** Immediate post-cardiac arrest 12-lead ECG displaying a global early repolarization pattern. **C.** Post-cardiac arrest 12-lead ECG displaying an inferolateral early repolarization pattern. **D.** Localization of the p. Val392Ile-KCND3 variant on the linear topology of the Kv4.3 voltage-gate potassium channel. **E.** Device EGM displaying the patient's first appropriate ventricular fibrillation-terminating (pre-quinidine) ICD therapy. **F.** Device EGM displaying the patient's second (after quinidine cessation for gastrointestinal symptoms/transaminitis) appropriate ventricular fibrillation-terminating ICD therapy.

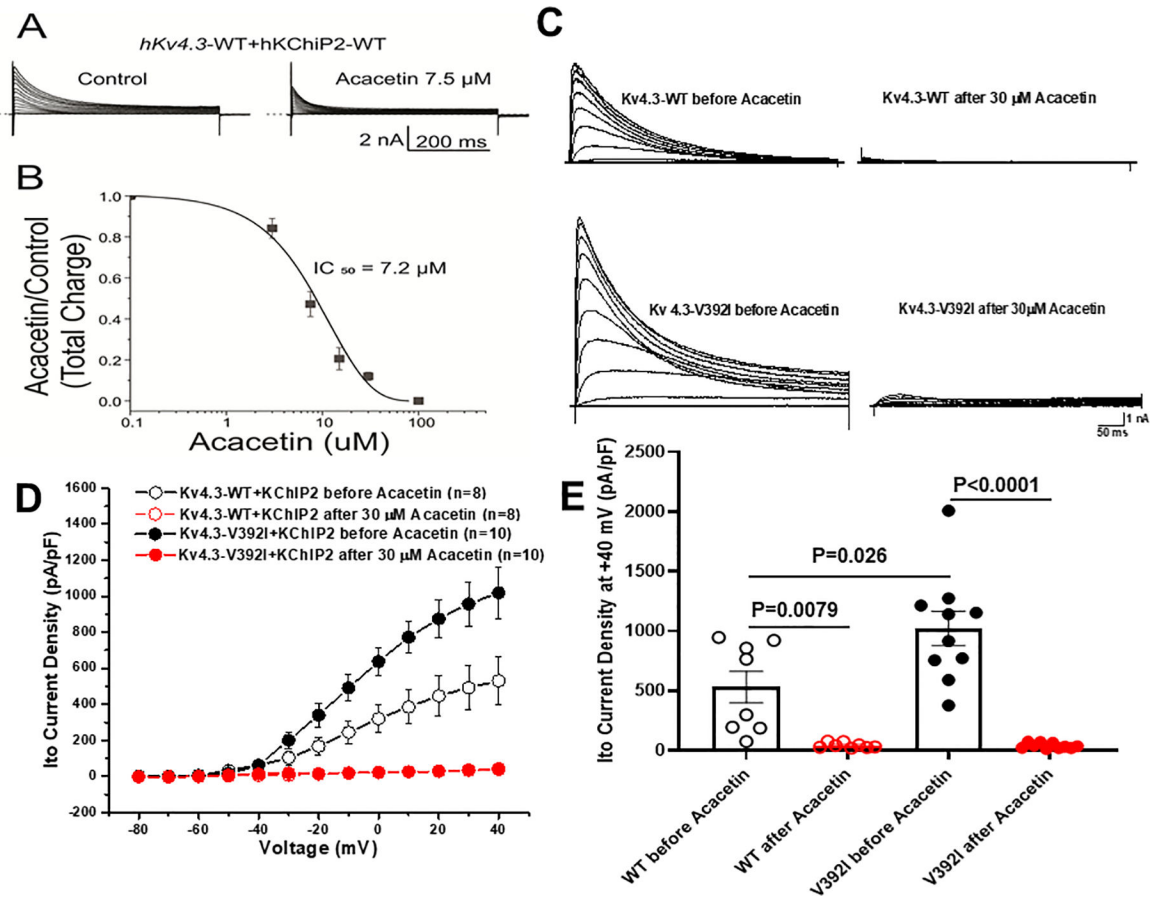


Figure 2.

Acacetin dramatically blocked I_{to} KCND3-WT and -V392I currents expressed in HEK293/TSA201 cells. **A**. Representative whole-cell Kv4.3-WT plus KChIP2-WT traces before and after 7.5 μM Acacetin from HEK293 cells. **B**. Concentration-response relationships for I_{to} total charge normalized to the current recorded at +50 mV under control and Acacetin conditions (room temperature). The IC_{50} value of Acacetin block of the I_{to} measured with KCND3-WT was $7.2 \pm 1.0 \mu\text{M}$ ($n=3-5$). **C**. Representative I_{to} KCND3-WT/V392I traces before and after 30 μM Acacetin from TSA201 cells elicited by step depolarization of 500 ms duration to +40 mV from a holding potential of -80 mV in 10 mV increments. **D**. The current voltage relationship for I_{to} KCND3-WT ($n=8$) and V392I ($n=10$) before and after 30 μM Acacetin. All values represent mean \pm SEM. **E**. Bar graph showing I_{to} peak current density at +40 mV for KCND3-WT ($n=8$) and V392I ($n=10$) before and after 30 μM Acacetin.

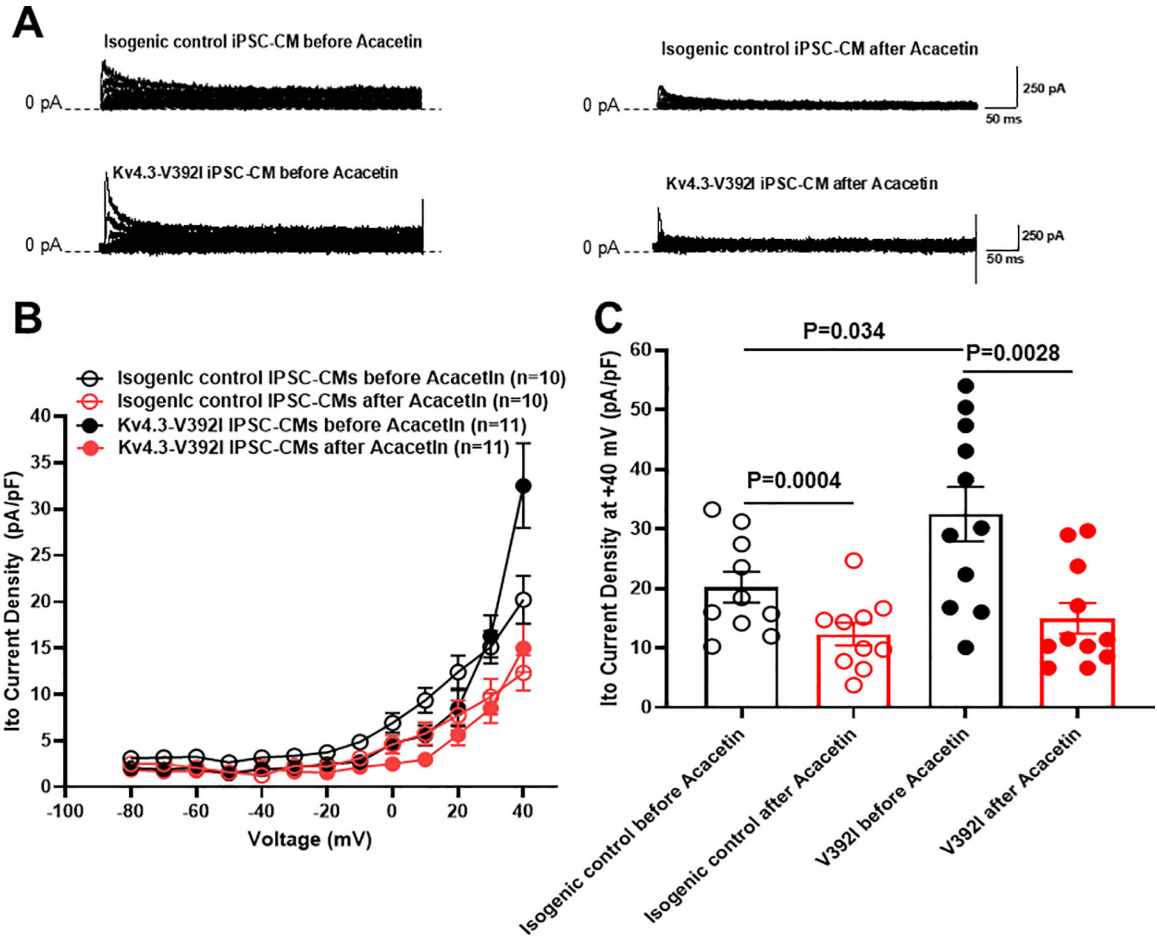


Figure 3. Acacetin significantly inhibited Ito currents from isogenic control and KCND3-V392i iPSC-CMs. **A.** Representative Ito traces before and after 10 μ M Acacetin from isogenic control and KCND3-V392i iPSC-CMs. **B.** The current voltage relationship for Ito from isogenic control (n= 10) and V392i (n=11) iPSC-CMs before and after 10 μ M Acacetin. All values represent mean \pm SEM. **C.** Bar graph showing Ito peak current density at +40 mV from isogenic control (n=10) and V392i (n=11) iPSC-CMs before and after 10 μ M Acacetin.

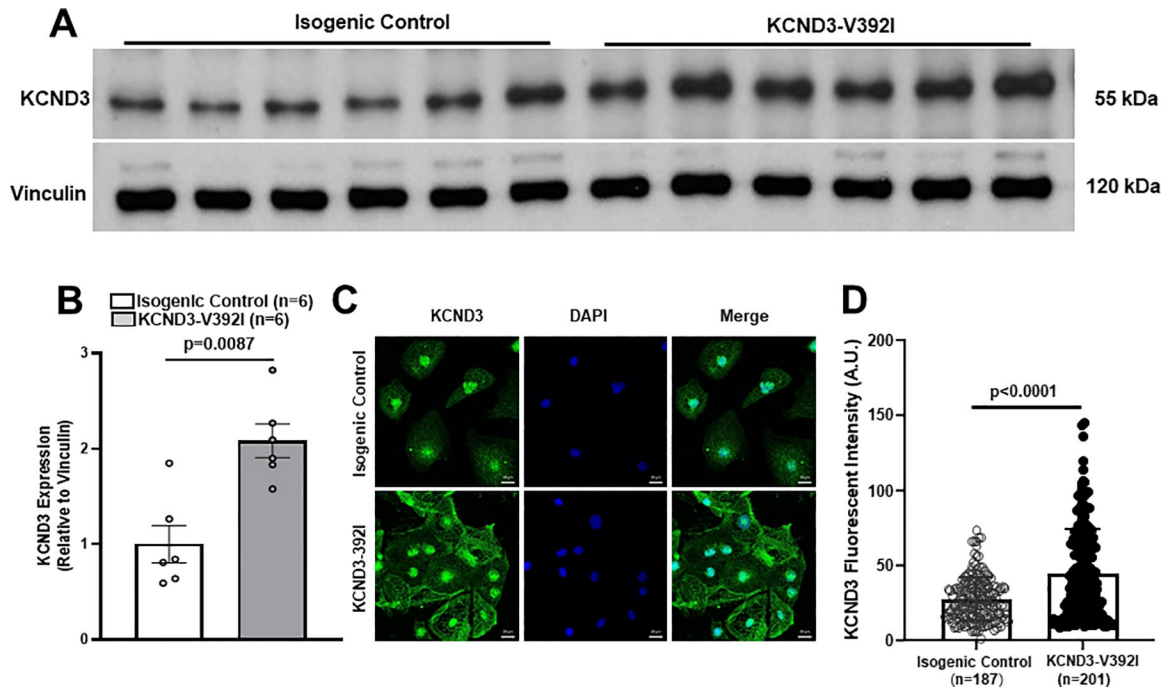


Figure 4.

KCND3 expression was significantly increased in KCND3-V392I iPSC-CMs. **A.** Western blot demonstrating KCND3 expression (relative to Vinculin) in isogenic control and KCND3-V392I iPSC-CMs. **B.** Bar graph showing KCND3 expression in isogenic control (n=6) and KCND3-V392I iPSC-CMs (n=6) by western blot data analysis. All values represent mean \pm SEM. Un-paired nonparametric (Mann-Whitney) test was used to determine statistical significance of KCND3 protein expression between two groups. **C.** Immunofluorescence study demonstrating KCND3 (green) localization in isogenic control and KCND3-V392I iPSC-CMs. Scale bars equal 20 μ m. **D.** Bar graph showing KCND3 fluorescent intensity in isogenic control (n=187) and KCND3-V392I iPSC-CMs (n=201). All values represent mean \pm SEM.

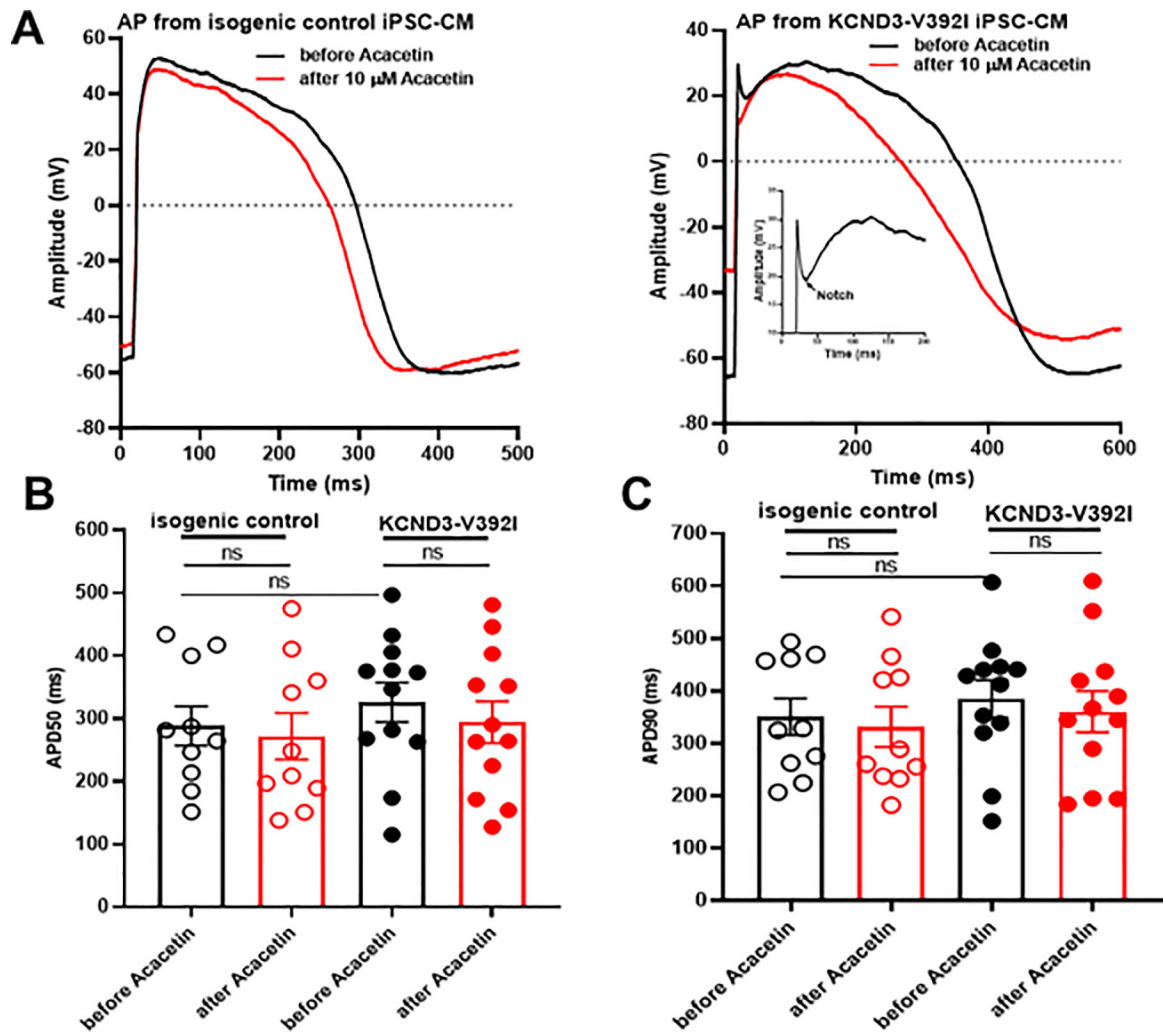


Figure 5.

Acacetin reduced accentuated AP notch in Kv4.3-V392I iPSC-CMs. **A.** Representative patch clamp AP traces before and after 10 μ M Acacetin from isogenic control and KCND3-V392I iPSC-CMs. **B.** Bar graph showing APD50 from isogenic control (n= 10) and V392I (n=12) iPSC-CMs before and after 10 μ M Acacetin. All values represent mean \pm SEM. ns represents no statistical significance. **C.** Bar graph showing APD90 from isogenic control (n= 10) and V392I (n=12) iPSC-CMs before and after 10 μ M Acacetin. All values represent mean \pm SEM. ns represents no statistical significance.

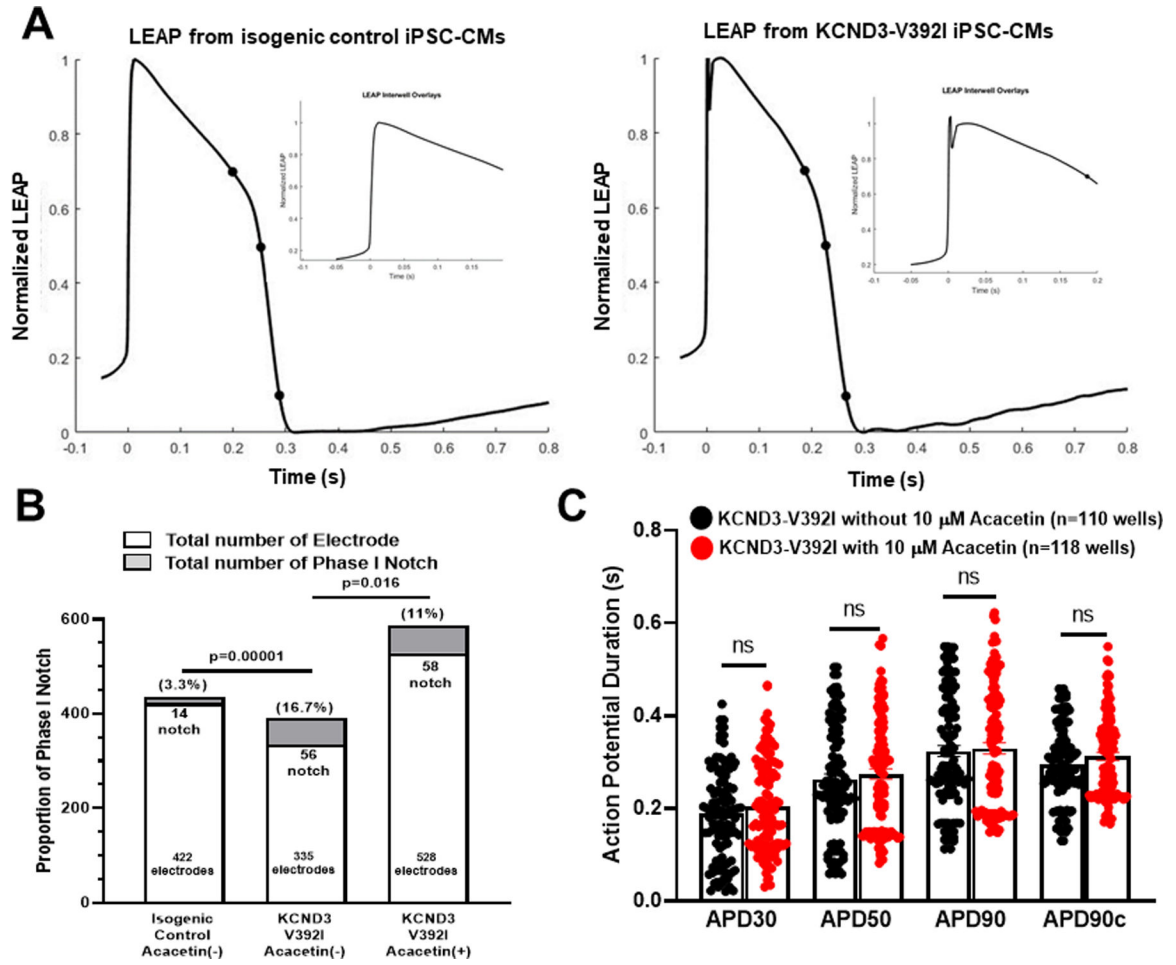


Figure 6.

Acacetin reduced total number of phase I notch in Kv4.3-V392I iPSC-CMs. **A.** Representative LEAP traces from isogenic control and KCND3-V392I iPSC-CMs. **B.** Bar graph showing LEAP proportion of phase I notch in isogenic control and KCND3-V392I iPSC-CMs without and with 10 μM Acacetin. Percentage of Phase I Notch among total electrodes in isogenic control vs. that in KCND3-V392I without Acacetin ($p=0.00001$), percentage of Phase I Notch among total electrodes in KCND3-V392I without Acacetin vs. that in KCND3-V392I with Acacetin ($p=0.016$). **C.** Bar graph showing LEAP APD30, APD50 and APD90 in KCND3-V392I iPSC-CMs without ($n=110$) and with ($n=118$) 10 μM Acacetin. All values represent mean±SEM. APD90 (Fridericia s) represents corrected APD90. ns represents no significant difference.